IOPscience iopscience.iop.org

Home Search Collections Journals About Contact us My IOPscience

# The influence of high energy proton bombardment on the electrical and defect properties of single-crystal ZnO

This article has been downloaded from IOPscience. Please scroll down to see the full text article.

2001 J. Phys.: Condens. Matter 13 8989

(http://iopscience.iop.org/0953-8984/13/40/315)

View the table of contents for this issue, or go to the journal homepage for more

Download details:
IP Address: 171.66.16.226
The article was downloaded on 16/05/2010 at 14:56

Please note that terms and conditions apply.

INSTITUTE OF PHYSICS PUBLISHING JOURNAL OF PHYSICS: CONDENSED MATTER
J. Phys.: Condens. Matter **13** (2001) 8989–8999 PII: S0953-8984(01)25533-7

# The influence of high energy proton bombardment on the electrical and defect properties of single-crystal ZnO

**F D Auret[1], S A Goodman[1], M Hayes[1], M J Legodi[1], H A van Laarhoven[1] and D C Look[2]**

[1] Physics Department, University of Pretoria, Pretoria 0002, South Africa
[2] Semiconductor Research Center, Wright State University, Dayton, OH, 45435, USA, and Materials and Manufacturing Directorate, Air Force Research Laboratory, OH 45433, USA

Received 6 June 2001
Published 20 September 2001
Online at stacks.iop.org/JPhysCM/13/8989

**Abstract**
We report on the electrical and defect characterization of Au Schottky diodes formed on single-crystal ZnO, before and after irradiating with high-energy (1.8 MeV) protons. Prior to bombardment we observed that several electron traps (E1–E4), with energies between 0.10 and 0.57 eV below the conduction band, are present in the ZnO. High-energy proton bombardment introduces two electron traps (Ep1 and Ep2), with extremely low introduction rates ($\eta$) of 2.4 and 1.9 cm$^{-1}$, respectively. Schottky barrier properties such as the reverse leakage current deteriorated from $1 \times 10^{-9}$ A for an unirradiated diode to $1 \times 10^{-6}$ A after bombarding it with a dose of $4.2 \times 10^{14}$ cm$^{-2}$ protons. Compared to GaN we found that ZnO is remarkably resistant to high-energy proton bombardment.

## 1. Introduction

ZnO, a wurtzitic semiconductor material with a high band gap, is presently used in many diverse products. It finds application in phosphors, paints, piezoelectric transducers, varistors and transparent conducting films, the latter being important for the photovoltaic industry. However, from a recent review, where the properties of ZnO are summarized [1], it is clear that ZnO can be used for several other, more sophisticated, electro-optical applications. Based on the fact that ZnO has an experimental direct band gap of 3.4 eV, it can play an important role in realizing blue and ultra-violet (UV) light emitting devices, such as light emitting diodes and lasers, as well as daylight-blind UV detectors, as is the case for GaN with a similar band gap. Furthermore, the large band gap of ZnO renders it suitable for the fabrication of solar cells, catalysts and as a substrate or buffer layer for the group III nitride based devices. For space applications, these devices often have to operate at elevated temperatures, typically above 200 °C, in harsh radiation conditions comprising energetic particles. Further practical

© 2001 IOP Publishing Ltd Printed in the UK

advantages of ZnO include bulk-growth capability, amenability to conventional wet chemistry etching, which is compatible with Si technology [2] (unlike the case for GaN), and convenient cleavage planes.

Other important considerations in the development of ZnO devices are the lack of good p-type material, and of a reliable Schottky-barrier (SB) fabrication technology. The latter problem not only precludes the realization of field-effect transistors, but also of capacitance-based characterization techniques, including capacitance–voltage ($C$–$V$) measurements, deep-level transient spectroscopy (DLTS) [3] and admittance spectroscopy (AS) [4]. (Note that electrochemical $C$–$V$ has been successful [5].)

Only a limited number of reports of ZnO characterization using DLTS and AS have appeared up to now. Most published reports on deep levels in ZnO focus on polycrystalline ZnO, and not on single crystals. Common to these reports is the presence of a defect, L2, with a level situated around 0.3 eV below the conduction band [6–11]. L2 has been proposed to be the oxygen vacancy [9]. A defect at 0.34 eV, as determined by temperature dependent Hall-effect measurements, could possibly be defect L2 [1]. Another defect, L1, with a level reported between 0.18 and 0.23 eV [8, 10, 12, 13], has only been observed in poly-ZnO, but little is known about its identity [6, 8, 10, 11]. Metal impurities were reported to introduce acceptor levels in the ZnO bandgap at $E_C - 0.17$ eV for Cu [12] and at $E_C - 0.23$ eV for Ag [13]. For a complete summary of the electronic properties of defects observed in ZnO by other authors the reader is referred to table 1.

**Table 1.** Literature survey of the electronic properties of prominent defects detected by DLTS in as-grown ZnO.

| Growth | $E_C - E_T$ (eV); $\sigma_n$ | Material details | Structure: technique |
|---|---|---|---|
| Sintered [6] | 0.138 (L1)<br>0.23 (L2)<br>(L3) | — | ZnO varistor: DLTS |
| Flux [7] | 0.3<br>0.17 (L1) | $N_D \sim 10^{16}$ cm$^{-3}$; $N_T \sim 10^{17}$ cm$^{-3}$ appears after 600 °C | Au/ZnO: AS |
| Sintered [8] | 0.26 (L2)<br>0.2–0.3 (L3) | $N_D = 0.8$–$1.5 \times 10^{17}$ cm$^{-3}$ | ZnO varistor: DLTS |
| Hydrothermal [9] | 0.28–0.32 (L2) | $N_D - N_A = 2$–$8 \times 10^{14}$ cm$^{-3}$ undoped ZnO | Au/ZnO & Ag/ZnO: DLTS |
| Sintered [10] | 0.24 (L1)<br>0.33 (L2)<br>0.18 (L1) | — | ZnO varistor: DLTS |
| Sintered [11] | 0.30 (L2)<br>0.36 (L3) | — | Varistor: DLTS |

An important consideration for space applications is that the material should be as radiation hard as possible in order for it to reliably operate for extended periods. Presently, the main wide-band-gap materials for space applications are considered to be the III–V nitrides, SiC and diamond. Whereas the effect of high-energy electron irradiation has been reported for ZnO [14], GaN [15, 16] and SiC [17], no data are yet available regarding the exposure of ZnO to heavier particles such as protons and He ions, as was reported for GaN [18, 19]. In particular, no data pertaining to radiation- and implantation-induced deep-level defects in ZnO are yet available. In the only report on the effect of high-energy electrons on ZnO, Look *et al* [14] concluded, from variable temperature Hall measurements, that the effect of these electrons on ZnO is significantly lower than that on GaN, GaAs and Si.

In this paper, we report on the electrical and defect characterization of single-crystal ZnO prior to and after high-energy proton bombardment. For capacitance-based characterization techniques (such as DLTS and $C$–$V$) it is necessary to fabricate good-quality Schottky barrier diodes (SBDs). For this study, Au SBDs were fabricated on the ZnO. DLTS reveals four defects (E1–E4) in the as-grown (unirradiated) material; after 1.8 MeV proton bombardment two additional electron trap defects are observed. The most significant observation was that ZnO is extremely radiation hard against high-energy protons compared to other wide-band-gap materials. For example, the free carrier removal rate by 1.8 MeV protons in ZnO is about 100 times less than that in GaN.

## 2. Experiment

The n-type ZnO used for this study was grown by a vapour-phase technique, making use of a nearly horizontal tube [20]. Following the cleaning procedure described before [21], circular Au contacts, 0.7 mm in diameter and 200 nm thick, were resistively deposited onto the $(000\bar{1})$ O face of the ZnO crystal through a mechanical mask. Thereafter, InGa ohmic contacts were applied to the opposite side (Zn face) of the sample. The Au/ZnO Schottky barrier diode (SBD) structures were characterized by standard room temperature (297 K) current–voltage ($I$–$V$) and $C$–$V$ measurements, and the defects in the ZnO by DLTS using a lock-in amplifier based system in the temperature range 25–330 K. $I$–$V$ measurements showed that the SBD had an ideality factor $n = 1.19$ (calculated by assuming that charge is predominantly transferred by thermionic emission) and a dark current of $10^{-9}$ A at a 1 V reverse bias. From $C$–$V$ measurements, the free carrier density, $N_D - N_A$, was found to vary, from sample to sample, between 4.6 and $5.6 \times 10^{16}$ cm$^{-3}$ in the first 0.2 $\mu$m below the SBD, i.e. the region being probed by DLTS.

After this characterization, the SBDs were bombarded at room temperature with 1.8 MeV protons in a Van de Graaff accelerator along the $[000\bar{1}]$ direction as well as 7 degrees off this direction. Bombardment at 7 degrees from a low-index crystallographic direction is the usual way to prevent channelling of the ions in the crystal (channelling of the ions can reduce the ion–atom collisions and so uncontrollably reduce the defect introduction). During bombardment, the dose rate was $1.4 \times 10^{11}$ protons cm$^{-2}$ s$^{-1}$ and the dose was incremented in steps of $1.4 \times 10^{14}$ cm$^{-2}$ up to a dose of $7.0 \times 10^{14}$ cm$^{-2}$. During irradiation, the temperature did not rise by more than a few °C. TRIM calculations indicated that the range of 1.8 MeV protons is about 19.5 $\mu$m and therefore only intrinsic defects, but no hydrogen, are introduced in the region probed by DLTS. After each irradiation step the SBDs and the ZnO were characterized by $I$–$V$, $C$–$V$ and DLTS. The diodes used for $I$–$V$ and $C$–$V$ measurements were not used for DLTS to ensure that their quality did not degrade due to the DLTS cooling and heating cycles.

The results of this study will be presented in two sections. The first deals with the electrical and defect properties of the Au/ZnO system prior to any bombardment (as grown), while the second section will present the results of similar measurements on the Au/ZnO system which has been bombarded with 1.8 MeV protons.

## 3. Results

### *3.1. As-grown material*

In order to accurately characterize defects present in the ZnO using DLTS prior to bombardment with high-energy protons, it is necessary to fabricate high-quality SBDs. Curve (a) of figure 1 depicts the room temperature forward and reverse current–voltage characteristics

of the Au/ZnO prior to bombardment. From this curve it is obvious that the Au diodes were of reasonable electrical quality and were suitable for DLTS analysis. A parameter of interest, the leakage current at 1.0 V reverse bias, is about $1 \times 10^{-9}$ A.

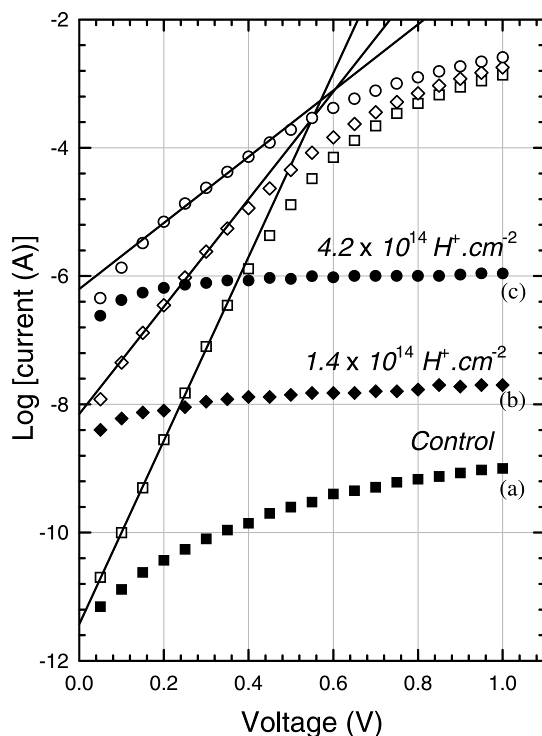


**Figure 1.** The current–voltage characteristics of Au/ZnO SBDs prior to bombardment with high-energy protons (curve (a)), and after a proton dose of $1.4 \times 10^{14}$ $H^+$ $cm^{-2}$ (curve (b)) and $4.2 \times 10^{14}$ $H^+$ $cm^{-2}$ (curve (c)). The filled symbols represent the reverse characteristics and the unfilled symbols the forward characteristics.

With the intent of establishing the activity of the shallow donors and the freeze-out conditions, we have performed thermally stimulated capacitance (TSCAP) measurements on Au/ZnO Schottky barrier diodes (SBDs) in the region 25–300 K. These measurements (curve (a) in figure 2, recorded at 6 K $min^{-1}$ while scanning up in temperature) showed that the capacitance, i.e. the number of ionized donors, reduces rapidly below 50 K. The derivative of the TSCAP with respect to temperature, shows where the Fermi level crosses the shallow donor level(s). This is consistent with the presence of shallow donor(s) as reported by Look *et al* [14].

Conventional lock-in amplifier (LIA) based DLTS in the temperature range 20–300 K (using the same SBDs) revealed the presence of at least three levels. From curve (b) in figure 2 (recorded at 46 Hz) we note that the peak of the first and most prominent defect, E1, occurs in the freeze-out region. This implies that an accurate analysis of its emission kinetics or concentration is not possible in this temperature region. Curve (a) of figure 3 illustrates the asymmetric DLTS peak of defect E1, recorded at a LIA frequency of 46 Hz. In an attempt to overcome this problem, DLTS spectra were recorded at a higher LIA (2200 Hz), where the E1 peak is observed above the freeze-out regime. From these measurements, we observed that the E1 peak is still quite asymmetric (curve (c) in figure 3). This indicates either that the E1

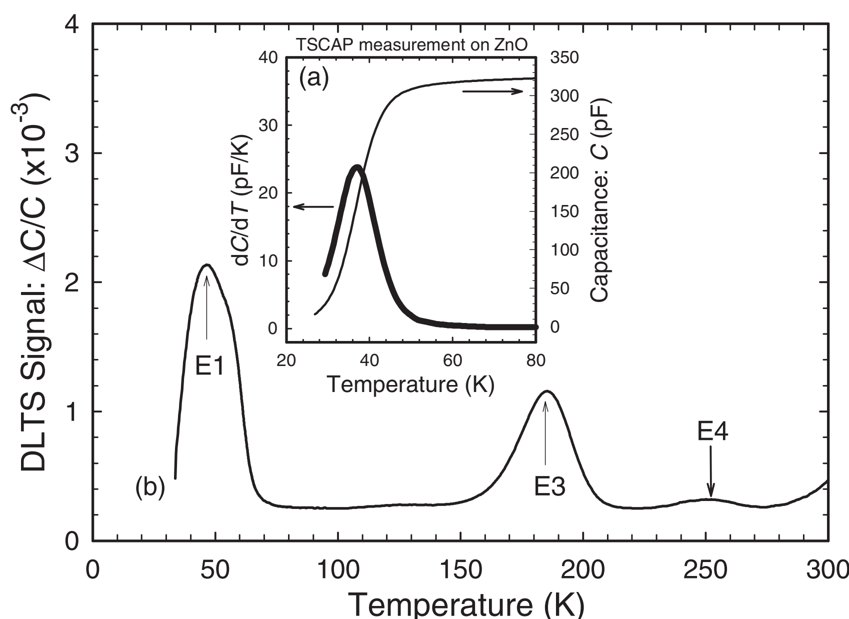


**Figure 2.** DLTS spectra of the control (prior to irradiation) Au/ZnO SBDs are depicted in curve (b), this spectrum was recorded using a LIA frequency of 46 Hz. The TSCAP recorded at 6 K $min^{-1}$ of Au/ZnO Schottky barrier diodes (SBDs) in the region 20–300 K is depicted in the inset.

peak is the superposition of more that one peak from closely spaced energy levels, or that it is the consequence of a strong electric field enhanced emission.

To assess the latter possibility, we recorded DLTS spectra for a constant reverse quiescent bias of 2 V using different filling pulse amplitudes in the range 0.1–2 V. These spectra (e.g. curve (b) in figure 3 at 2200 Hz) revealed that the peak shape of E1 is almost symmetric for low filling pulse values (i.e. low electric fields), as is to be expected for emission from a single, well defined energy level. However, the peak shape of E1 distorts strongly towards low temperatures with increasing filling pulse amplitude (i.e. increasing electric field). This is typical of electric field enhanced emission where the electric field enhances emission of carriers from the potential well, either by distorting the well so that its effective barrier is reduced (Poole–Frenkel effect [22]), or by phonon assisted tunnelling or pure tunnelling. Whereas the Poole–Frenkel effect is indicative of emission from a charged well (i.e. a donor-like defect in n-type material), the other mechanisms may occur from neutral wells.

Using the lowest possible electric field that still yields a strong enough signal for DLTS measurements ($V_r = 2$ V and $V_p = 0.1$ V), we determined the activation energy and apparent capture cross section of E1 as 0.12 eV and $2 \times 10^{-13}$ $cm^2$, respectively (table 2 and figure 4). No defect with a similar energy has yet been reported in the literature, possibly because all previous DLTS and AS measurements were performed in liquid nitrogen based (77 K) cryostats. The fixed bias–variable pulse DLTS method was used to determine the concentration profile of E1, which indicated that its concentration is about $10^{16}$ $cm^{-3}$ in the region probed by DLTS. It should be mentioned that the extreme sensitivity of E1 to the electric field made it difficult to obtain an accurate depth profile.

The peak position of the second most prominent level, E3, exhibited very little dependence on the electric field. We have determined its activation energy and apparent capture cross-section as 0.29 eV below the conduction band and $6 \times 10^{-16}$ $cm^2$, respectively (table 2 and

**Table 2.** Electronic properties of prominent defects detected by DLTS in as-grown and 1.8 MeV proton-bombarded single-crystal n-type ZnO.

| Defect label | $E_T$ (eV) | $\sigma_a$ ($cm^2$) | $N_T$ ($cm^{-3}$) | $T^{a}_{peak}$ (K) | Similar defects and references |
|---|---|---|---|---|---|
| E1 | $0.12 \pm 0.02$ | $2.7 \pm 1.0 \times 10^{-13}$ | $\approx 10^{16}$ | $70^{b}$ | |
| E3 | $0.29 \pm 0.01$ | $5.8 \pm 1.0 \times 10^{-16}$ | $10^{14}$ | 184 | L3? [12] |
| E4 | $0.57 \pm 0.02$ | $2.0 \pm 0.5 \times 10^{-12}$ | $10^{13}$–$10^{14}$ | 249 | |
| | | | $\eta$ ($cm^{-1}$) | | |
| Ep1 | $0.54 \pm 0.02$ | $3.0 \pm 1.0 \times 10^{-13}$ | $2.4 \pm 0.5$ | 251 | E4 [10] |
| Ep2 | $0.78 \pm 0.02$ | $1.5 \pm 0.5 \times 10^{-12}$ | $1.9 \pm 0.4$ | $304^{c}$ | |

[a] Peak temperature at a lock-in amplifier frequency of 46 Hz (emission rate of 109 $s^{-1}$).
[b] Peak temperature at a lock-in amplifier frequency of 2200 Hz (emission rate of 5200 $s^{-1}$).
[c] Peak temperature at a lock-in amplifier frequency of 2.2 Hz (emission rate of 5.2 $s^{-1}$).

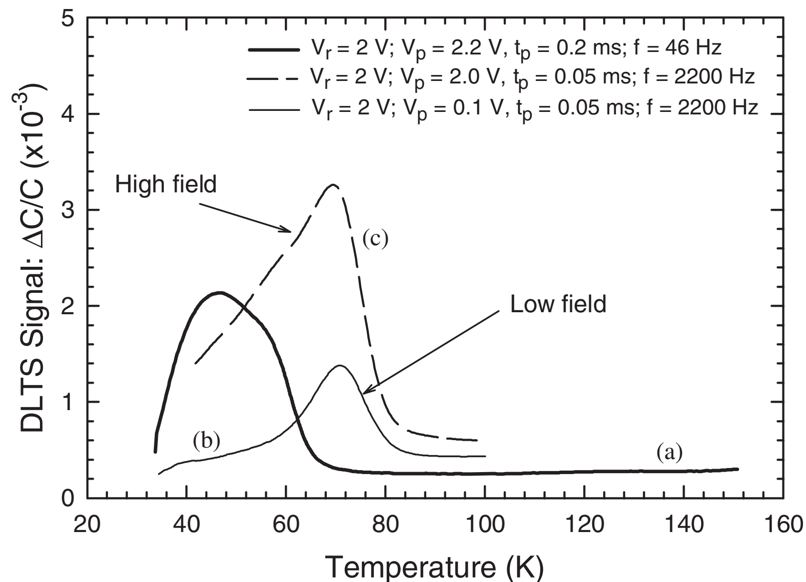


**Figure 3.** DLTS spectra of the as-grown defect E1. Curve (a) recorded at a LIA frequency of 46 Hz depicts the asymmetric peak recorded in the vicinity of the freeze-out region. Curves (b) and (c) were recorded at 2200 Hz at a low and a high electric field respectively.

figure 4). The concentration of E3, determined by DLTS profiling, was found to be about $10^{14}$ $cm^{-3}$. This together with its small apparent capture cross section indicates that it may be an acceptor-like defect. The DLTS signature of E3 is similar to that of the L2, previously speculated to be the oxygen vacancy [9].

A third, less prominent defect, E4, is present in a concentration of $10^{13}$–$10^{14}$ $cm^{-3}$. Its concentration varied from sample to sample. We have determined the activation energy and apparent capture cross section of E4 as 0.59 eV below the conduction band and $2 \times 10^{-12}$ $cm^2$, respectively (table 2 and figure 4). The unrealistically high value of its apparent capture cross section suggests that E4 may not be a simple point defect. No defect with a similar energy has

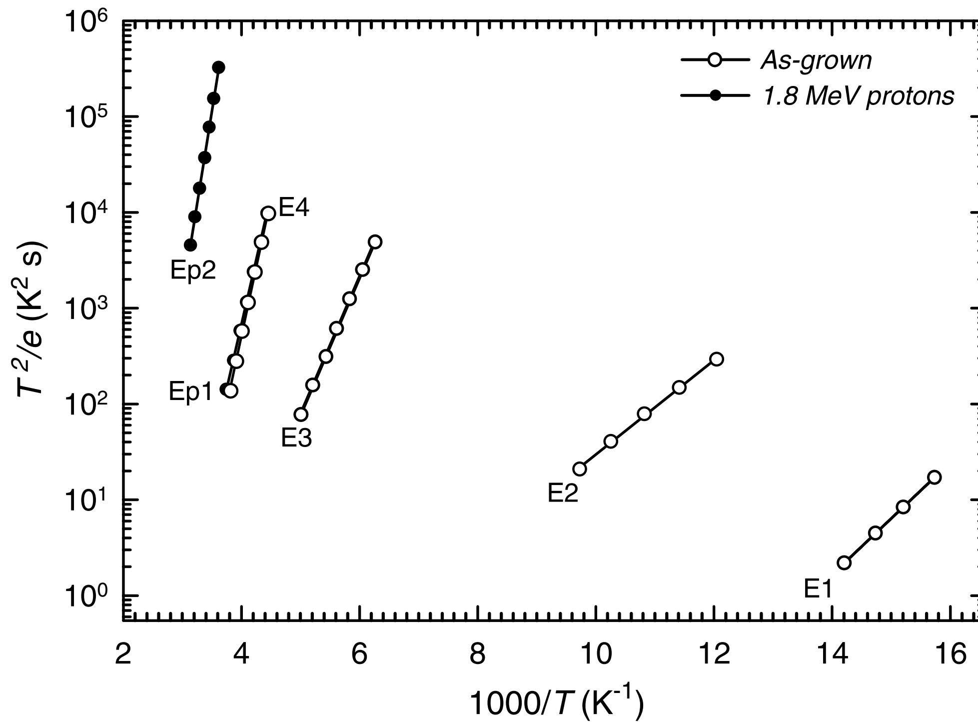


**Figure 4.** Arrhenius plot of defects (E1–E4) observed in as-grown single-crystal ZnO (unfilled symbols) and those defects (Ep1, Ep2) observed after 1.8 MeV proton bombardment (filled symbols).

yet been reported in the literature. Another minor peak, E2, not observed in all samples, was found to have an activation energy and apparent capture cross section of 0.10 eV below the conduction band and $1 \times 10^{-17}$ cm$^2$, respectively.

### 3.2. Proton bombarded ZnO

From the $I$–$V$ measurements illustrated in curves (b) and (c) of figure 1, it can be seen that proton bombardment degrades the diode quality. For example, the reverse current at a bias of 1 V ($I_R$) increased from $1 \times 10^{-9}$ A for an unirradiated diode to $1 \times 10^{-6}$ A after bombarding it with a dose of $4.2 \times 10^{14}$ cm$^{-2}$. Both the forward and reverse $I$–$V$ characteristics appeared to have a generation–recombination (RG) nature after bombardment. This indicates that proton irradiation introduces deep defect levels in the band-gap of ZnO.

The most surprising results obtained here were from $C$–$V$ measurements. In figure 5 we depict the free carrier concentration, $N_D - N_A$, as function of proton dose. From the data in this figure we see that a dose, $D$, of $7.0 \times 10^{14}$ cm$^{-2}$ reduces $N_D - N_A$ by $2.49 \times 10^{16}$ cm$^{-3}$. From these data, the free carrier removal rate

$$\zeta = \frac{\Delta(N_D - N_A)}{D} \tag{1}$$

was calculated as $35 \pm 3.6$ cm$^{-1}$ for irradiation along the $[000\bar{1}]$ direction. For bombardment 7 degrees off the $[000\bar{1}]$ direction, the value of $\zeta$ increased to $45 \pm 4.5$ cm$^{-1}$. The value of

$\zeta$ calculated here is about 100 times lower than that of GaN bombarded by 1.0 MeV protons. At this point it should be noted that Look *et al* also observed a very small change in the free carrier density of ZnO after high-energy electron irradiation [14]. Possible reasons for this low carrier removal rate will be discussed after presenting the DLTS results.

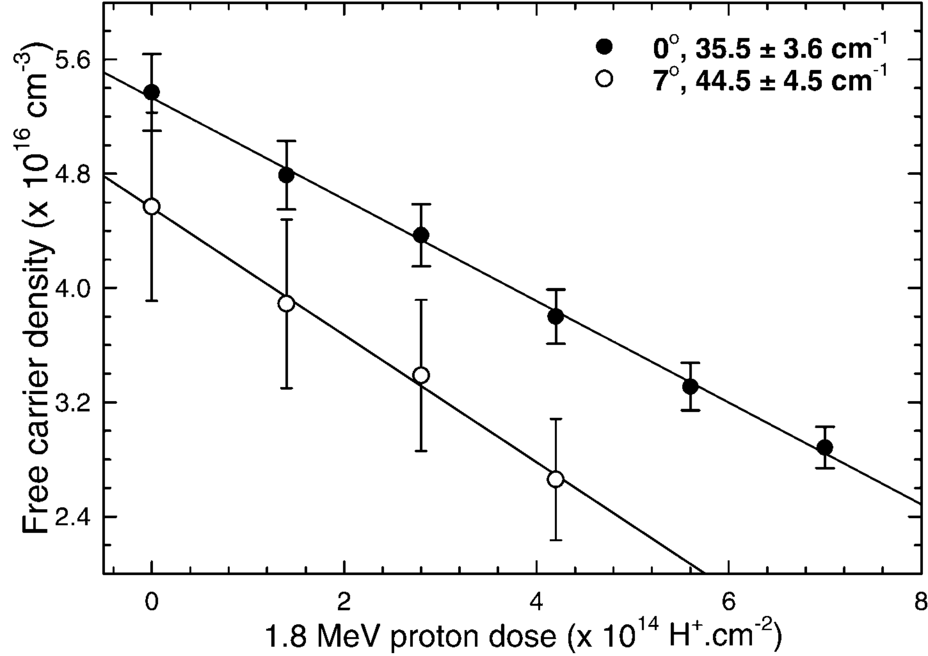


**Figure 5.** Free carrier density, $N_D - N_A$ (at 0.2 $\mu$m below the interface) determined from $C$–$V$ measurements as a function of 1.8 MeV proton dose incident at 0° (filled symbols) and 7° (unfilled symbols) with the $[000\bar{1}]$ axis.

After proton bombardment two additional electron traps are observed. Curve (b) in figure 6 shows that proton bombardment introduces at least two electron traps with peaks in the temperature region scanned by DLTS. The first of these defects, Ep1, has an energy level, $E_T$, and apparent capture cross-section, $\sigma_a$, of 0.54 eV and $3 \times 10^{-13}$ cm$^2$, respectively. This DLTS signature of Ep1 is similar, within the experimental error, to that of the E4 defect (with unknown origin) detected in low concentrations in unirradiated ZnO (curve (a)). The second defect introduced by proton irradiation, Ep2, was not detected in the unirradiated ZnO and has a signature of $E_T = 0.78$ eV and $\sigma_a = 1.5 \times 10^{-12}$ cm$^2$. It is further instructive to note that Ep2 is located deep enough below the conduction band to contribute to generation currents during $I$–$V$ measurements.

DLTS depth profiling was employed to measure the concentration profiles of the proton irradiation induced defects after each irradiation step. The defect concentrations at 0.2 $\mu$m below the junction are plotted in the inset of figure 6 as a function of proton dose. From these data the defect introduction rate, $\eta$, for each defect was calculated from

$$\eta = \frac{\Delta N_T}{D} \tag{2}$$

where $\Delta N_T$ is the increase in defect concentration for a dose $D$. The values of $\eta$ for Ep1 and Ep2 thus calculated are $2.4 \pm 0.5$ cm$^{-1}$ and $1.9 \pm 0.4$ cm$^{-1}$, respectively. These introduction rates are more than one order of magnitude lower than those for defects detected in any other

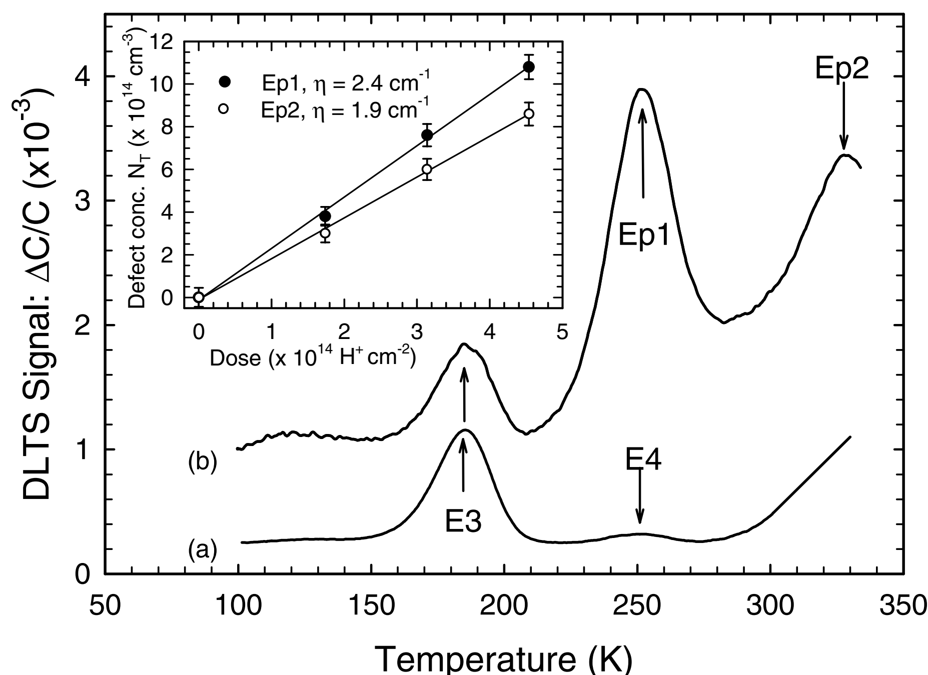


**Figure 6.** DLTS spectra of control Au/ZnO SBDs (curve (a)) and similar SBDs that were bombarded with 1.8 MeV protons to a dose of $4.2 \times 10^{14}$ cm$^{-2}$ (curve (b)). All spectra were recorded using a quiescent reverse bias of 2 V, a filling pulse amplitude of 2.2 V, a lock-in amplifier frequency of 46 Hz (i.e. a decay time constant of 9.23 ms) and a filling pulse width of 0.2 ms. The inset depicts the defect concentrations of Ep1 and Ep2 (at 0.2 $\mu$m below the interface) as a function of the 1.8 MeV proton dose.

semiconductor implanted with protons having a similar energy at room temperature. For example, in GaN with a similar band-gap, the major radiation induced defect, with an energy level at $E_T = E_C - 0.20$ eV, is introduced at a rate of about 30 cm$^{-1}$ by MeV protons.

## 4. Discussion

Two main questions arise from results presented here. Firstly, what is the nature of the defects in the as-grown ZnO?, and secondly, why is the defect introduction rate, and together with that, the free carrier removal rate, so much lower in ZnO than in other semiconductors, some of which have similar crystal structures and atomic densities (for example GaN)? To obtain an answer to the first question, spectroscopic studies should be correlated with DLTS and AS measurements. There are at least two possible solutions to the second question that have to be explored. Firstly, the primary defects introduced in ZnO during proton bombardment may be mobile at room temperature (where the irradiation was performed) and, therefore, they may anneal out. In this case these defects and their effect on the free carrier density, will therefore not be detected by DLTS or $C$–$V$ measurements. The defects, Ep1 and Ep2, that we observed may therefore be second-generation defects of which the introduction rates are much lower than those of the primary radiation induced defects. A similar situation prevails in Si, where vacancies and interstitials anneal out at low temperatures and the second-generation defects (divacancies and vacancy–impurity

complexes) detected after room-temperature irradiation are observed at lower introduction rates [23]. This possibility will have to be investigated by irradiating ZnO at low temperatures and measuring the value of $N_D - N_A$, as well as the DLTS spectrum, as a function of increasing temperature.

The second possibility is that the defects detected here, Ep1 and Ep2, are not the main radiation induced defects in ZnO. The main radiation induced defects may be pairs of shallow donors (too shallow to be detected by DLTS) and deep acceptors (too deep to be detected by DLTS), that are introduced in roughly equal concentrations. Since the number of shallow donors introduced by radiation will balance the number of radiation induced acceptors, we will not observe any drastic change in the free carrier concentration and neither will we detect any major DLTS peaks in the temperature domain investigated. This possibility will have to be verified by performing admittance spectroscopy measurements to facilitate the detection of defect levels too deep to be detected by DLTS, and Hall and photoluminescence measurements to detect the shallow donors (too shallow to be detected by DLTS). At this point it should be noted that Look *et al* have reported an increase in concentration of one of the shallow donors in ZnO after electron irradiation [14].

## 5. Conclusions

In summary, our DLTS results revealed the presence of a semi-shallow defect ($E_T = E_C - 0.12$ eV) in as-grown single-crystal ZnO. This defect has not been observed before with any junction spectroscopic technique. In addition, by using $C$–$V$ and DLTS measurements, we have demonstrated that ZnO is extremely resistant to room-temperature MeV proton irradiation when compared to other semiconductors, including GaN. The consequence of this is extremely important: ZnO can be used for space applications (where it will be exposed to inherently harsh radiation conditions) for much longer periods of time than any other semiconductor with similar electro-optical properties before becoming useless due to radiation damage. One possible explanation for the extreme radiation hardness of ZnO is that the primary radiation induced defects in it may be unstable at room temperature and that they anneal out before forming harmful compensating centres.

## Acknowledgments

We gratefully acknowledge financial assistance of the South African National Research Foundation (NRF) and Eagle-Picher Technologies, LLC, for supplying the ZnO used for this study. DCL was supported by US Air Force Contract F33615-00-C-5402.

## References

[1] Look D C 2001 *Mater. Sci. Eng.* B **80** 383
[2] Vellekoop M J, Visser C C G, Sarro P M and Venema A 1990 *Sensors Actuators* A **21–23** 1027
[3] Lang D V 1974 *J. Appl. Phys.* **45** 3023
[4] Vincent G, Bois D and Pinard P 1975 *J. Appl. Phys.* **46** 5173
[5] Stutz C E 2000 private communication
[6] Lee W-I, Young R-L and Chen W-K 1996 *Japan. J. Appl. Phys.* **35** L1158
[7] Kanai Y 1990 *Japan. J. Appl. Phys.* **29** 1426
[8] Rohatgi A, Pang S K, Gupa T K and Straub W D 1988 *J. Appl. Phys.* **63** 5375
[9] Simpson J C and Cordaro J F 1988 *J. Appl. Phys.* **63** 1781
[10] Shohata N, Matsumura T and Ohno T 1980 *Japan. J. Appl. Phys.* **19** 1793
[11] Nitayama A, Sakaki H and Ikoma T 1980 *Japan. J. Appl. Phys.* **19** L743

[12] Kanai Y 1991 *Japan. J. Appl. Phys.* **30** 703
[13] Kanai Y 1991 *Japan. J. Appl. Phys.* **30** 2021
[14] Look D C, Reynolds D C, Hemsky J W, Jones R L and Sizelove J R 1999 *Appl. Phys. Lett.* **75** 811
[15] Fang Z-Q, Look D C, Kim W, Fan Z, Botchkarev A and Morkoc H 1998 *Appl. Phys. Lett.* **72** 2277
[16] Goodman S A, Auret F D, Legodi M J, Gibart P and Beaumont B 2001 *Appl. Phys. Lett.* submitted
[17] Hallen A, Henry A, Pellegrino P, Svensson B G and Åberg D 1999 *Mater. Sci. Eng.* B **61/62** 378
[18] Auret F D, Goodman S A, Koschnick F K, Spaeth J-M, Beaumont B and Gibart P 1999 *Appl. Phys. Lett.* **74** 407
[19] Auret F D, Goodman S A, Koschnick F K, Spaeth J-M, Beaumont B and Gibart P 1998 *Appl. Phys. Lett.* **73** 3745
[20] Look D C, Reynolds D C, Sizelove J R, Jones R L, Litton C W, Cantwell G and Harsch W C 1998 *Solid State Commun.* **105** 399
[21] Auret F D, Goodman S A, Legodi M J, van Laarhofen H A and Look D C 2001 *Appl. Phys. Lett.* submitted
[22] Frenkel J 1939 *Phys. Rev.* **54** 657
[23] Troxell J R 1983 *Solid-State Electron.* **26** 539